Electronic Supplementary Material (ESI) for RSC Advances.

$Zn_3V_2O_7(OH)_2 \cdot 2H_2O$/MXene Cathode with fast ion diffusion for Highly Durable Zinc Ion Battery

Wanting Su†, Man Lang†, Weiwei Li, Huili Li*

The Education Ministry Key Lab of Resource Chemistry, Shanghai Key Laboratory of Rare Earth Functional Materials, College of Chemistry and Materials Science, Shanghai Normal University, Shanghai 200234, P. R. China.

*E-mail: li_huili@shnu.edu.cn

†Wanting Su and Man Lang contributed equally to this work.

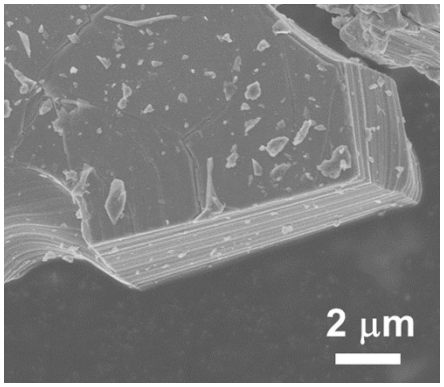

Figure S1 SEM image of Ti_3AlC_2 MAX.

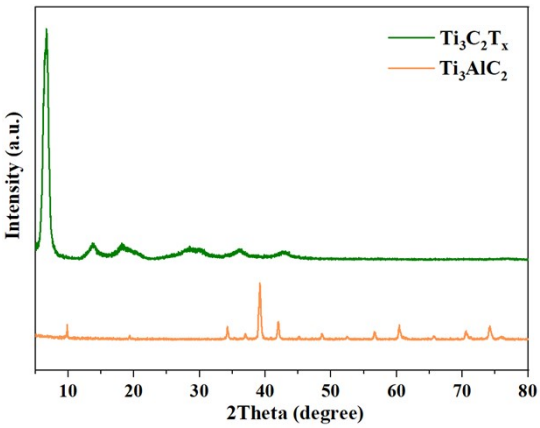

Figure S2 XRD patterns of Ti_3AlC_2 and $Ti_3C_2T_x$ MXene.

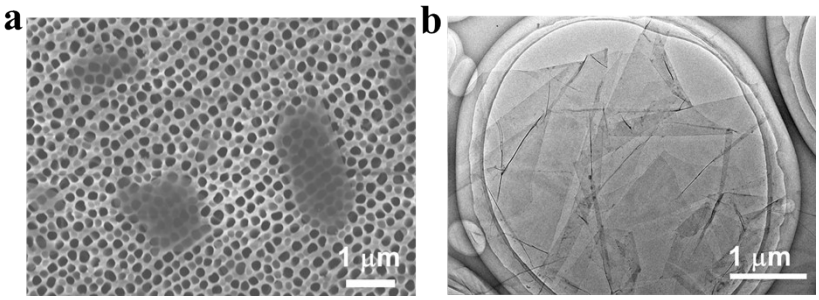

Figure S3 (a) SEM and TEM image of $Ti_3C_2T_x$ MXene.

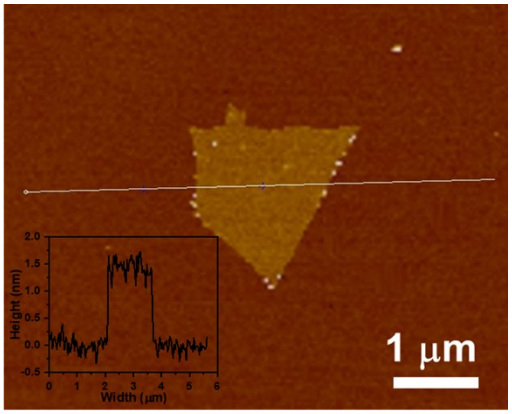

Figure S4 Atomic Force Microscope of $Ti_3C_2T_x$ MXene.

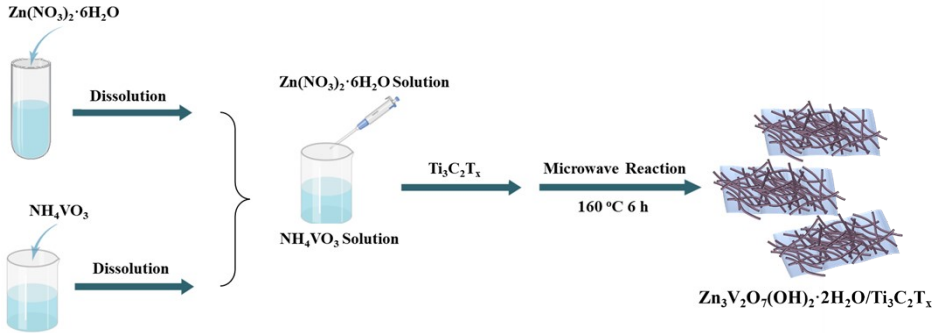

Figure S5 The synthesis process of ZVO/$Ti_3C_2T_x$ composites.

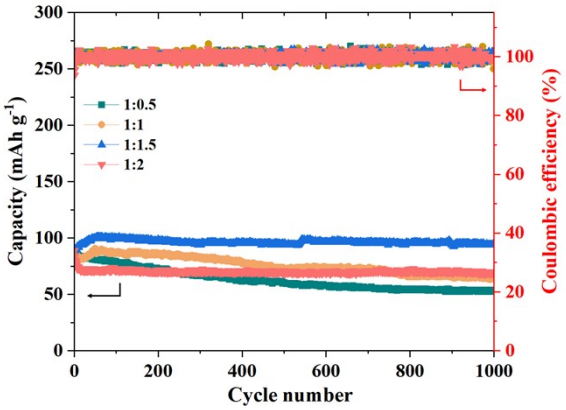

Figure S6 The cycling stability of ZVO/$Ti_3C_2T_x$ electrodes synthesized from different molar ratio of NH_4VO_3 and $Zn(NO_3)_2·6H_2O$.

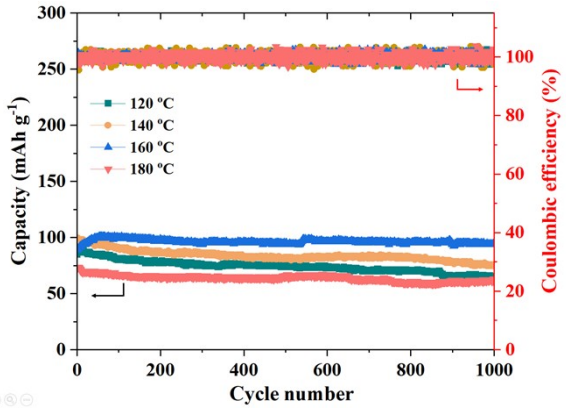

Figure S7 The cycling stability of ZVO/$Ti_3C_2T_x$ electrodes synthesized from different microwave reaction temperature.

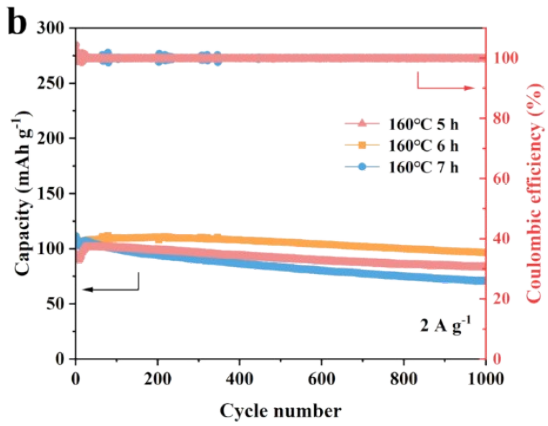

Figure S8 The cycling stability of ZVO/$Ti_3C_2T_x$ electrodes synthesized from different microwave reaction time.

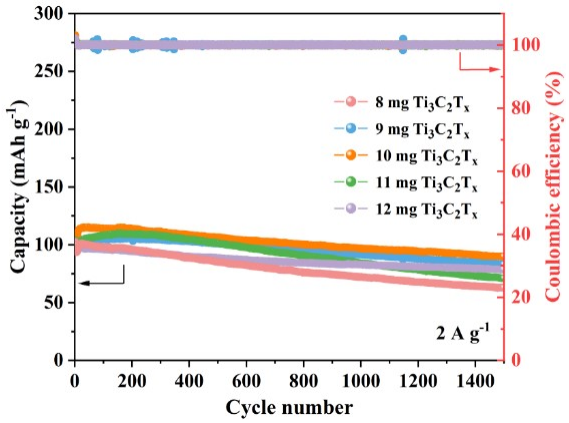

Figure S9 The cycling stability of ZVO/$Ti_3C_2T_x$ electrodes synthesized from different mass of $Ti_3C_2T_x$.

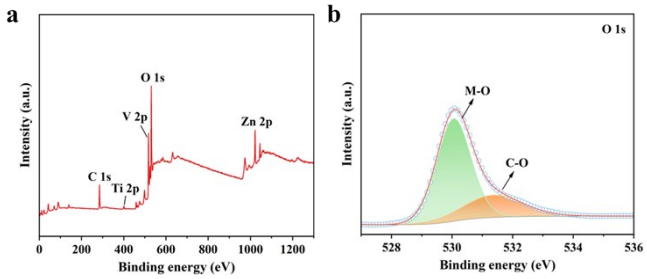

Figure S10 (a) XPS spectrum of ZVO/$Ti_3C_2T_x$ MXene. (b) The high-resolution XPS spectrum of O 1s in the (a).

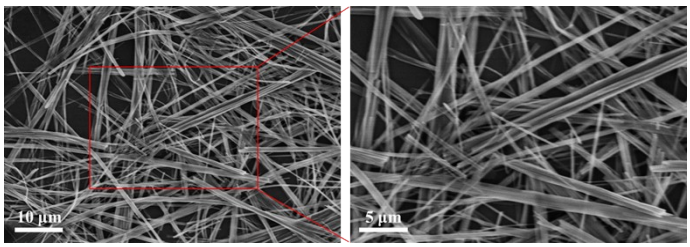

Figure S11 SEM images of ZVO.

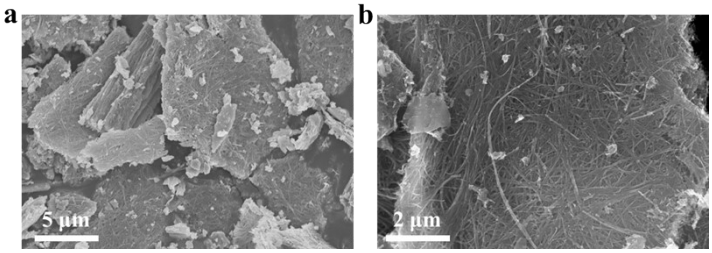

Figure S12 SEM images ZVO/$Ti_3C_2T_x$ composites.

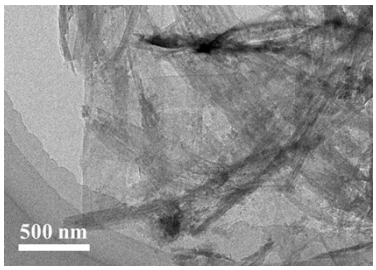

Figure S13 TEM image of ZVO/$Ti_3C_2T_x$ composites.

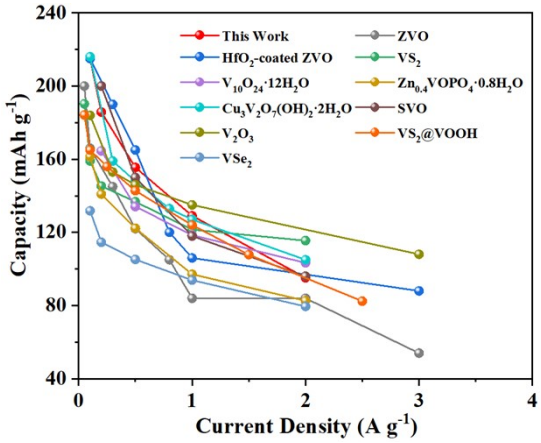

Figure S14 The capacity of Zn//ZVO/$Ti_3C_2T_x$ batteries compared with the values reported of other similar vanadium-based ZIBs.

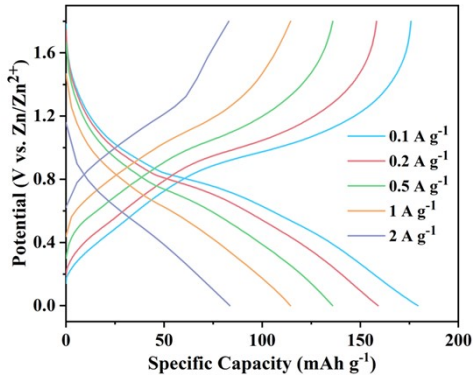

Figure S15 The galvanotactic charge/discharge curves Zn//ZVO batteries under various current densities.

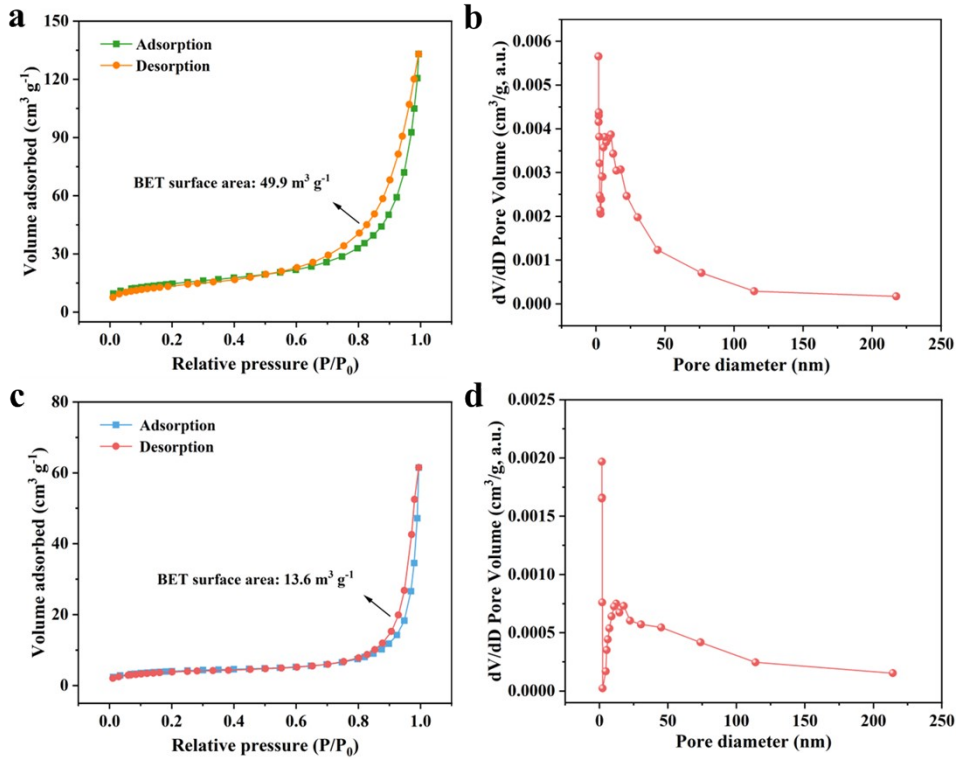

Figure S16 (a) Nitrogen adsorption/desorption isotherms and (b) pore size distribution curves of ZVO/$Ti_3C_2T_x$. (a) Nitrogen adsorption/desorption isotherms and (b) pore size distribution curves of $Zn_3V_2O_7(OH)_2$.

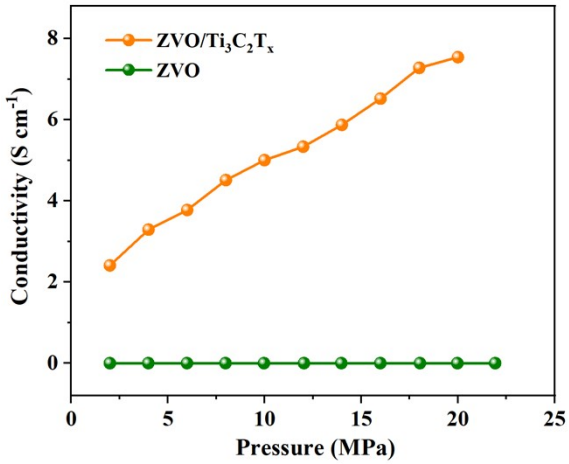

Figure S17 Electronic conductivity of ZVO/$Ti_3C_2T_x$ and ZVO.

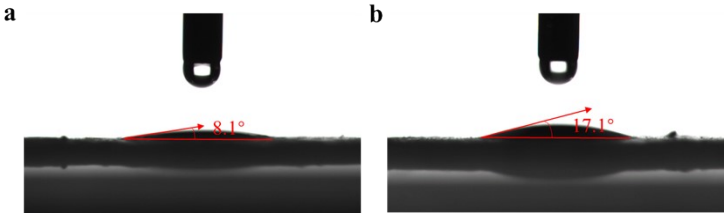

Figure S18 Water contact angles of (a) ZVO/$Ti_3C_2T_x$ and (b) ZVO.

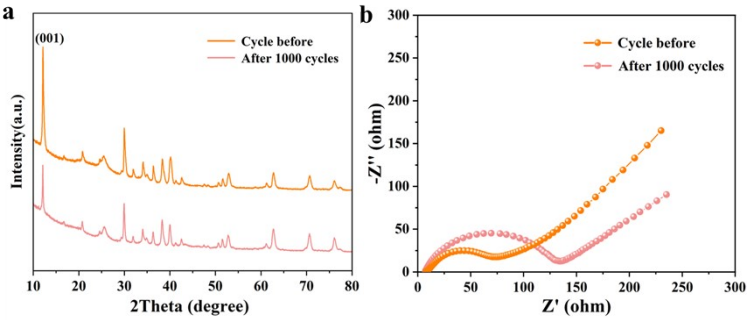

Figure S19 (a) XRD and (b) Electrochemical impedance spectroscopy spectra of Zn//MoS_2/$Ti_3C_2T_x$ batteries before and after charge/discharge cycles.

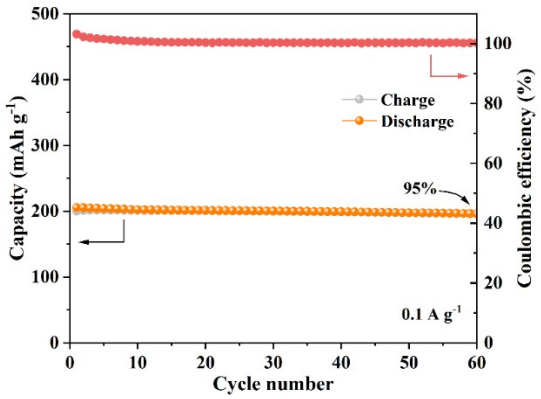

Figure S20 Long cycling performance of Zn//ZVO/$Ti_3C_2T_x$ batteries at 0.1 A g^{-1}.

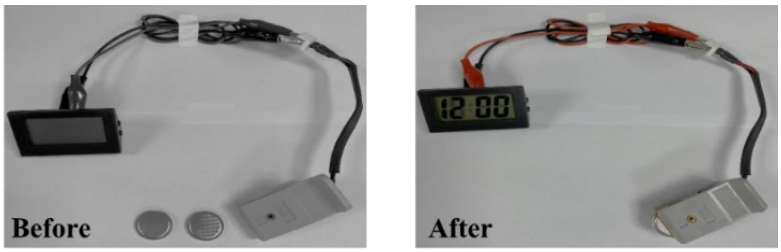

Figure S21 Digital photographs of Zn//ZVO/$Ti_3C_2T_x$ batteries in series to power a

clock.

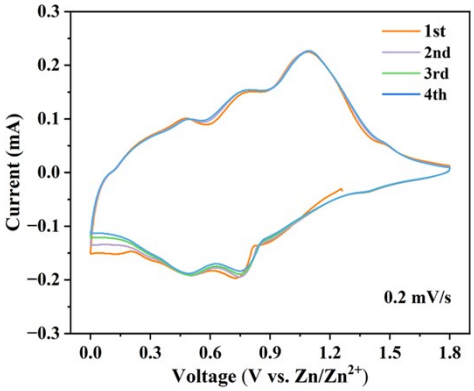

Figure S22 Cyclic voltammogram profiles of Zn//ZVO/$Ti_3C_2T_x$ batteries at different scan cycles.

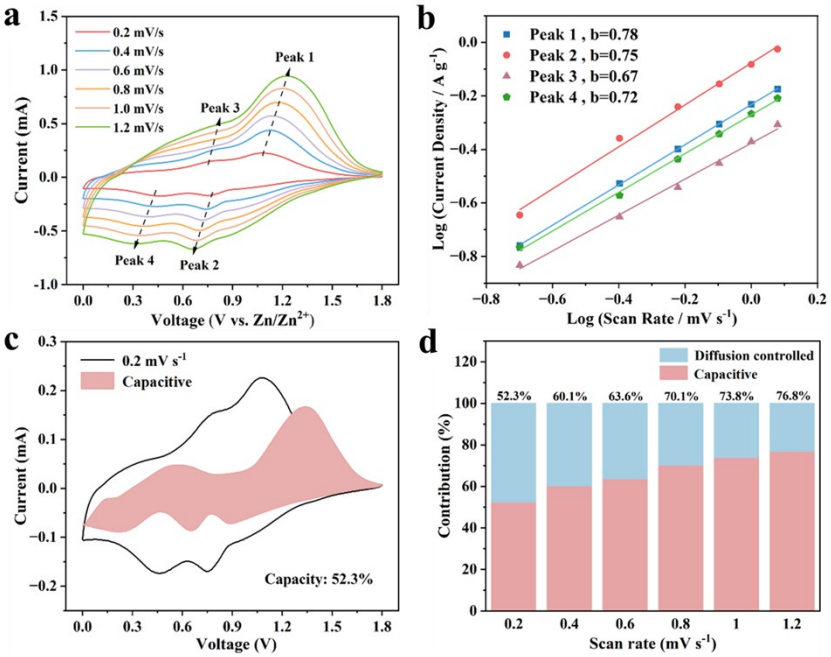

Figure S23 (a) Cyclic voltammogram profiles of Zn//ZVO batteries at various scan rates. (b) The fitting plots between log(i) and log(v) at various peak currents. (c) Quantification of the capacitive (red area) and diffusion charge storage in the ZVO/$Ti_3C_2T_x$ electrode at a scan rate of 0.2 mV s^{-1} and (d) the ratio of the capacitive contribution (red) to the diffusion contribution (blue) as a function of scan rate.

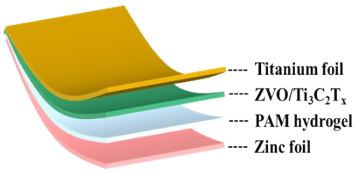

Figure S24 Scheme of flexible ZIBs based on ZVO/$Ti_3C_2T_x$ composites.

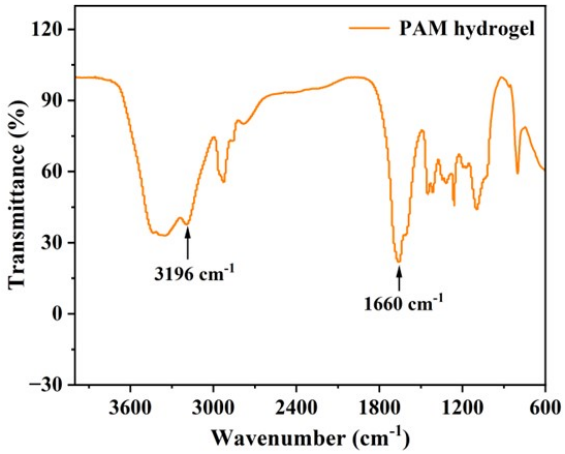

Figure S25 FT-IR spectra of PAM hydrogel.

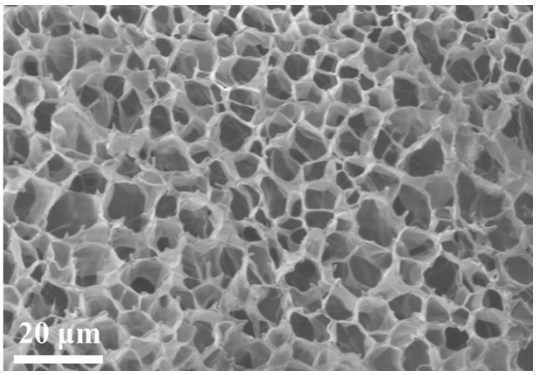

Figure S26 SEM images of PAM hydrogel.

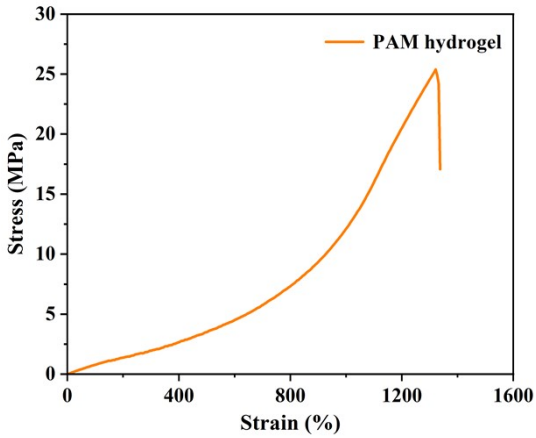

Figure S27 Stress-strain curve of PAM hydrogel.

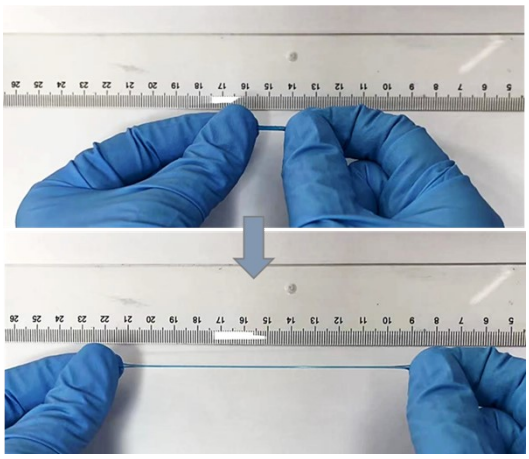

Figure S28 Digital photographs of stretched PAM hydrogel.

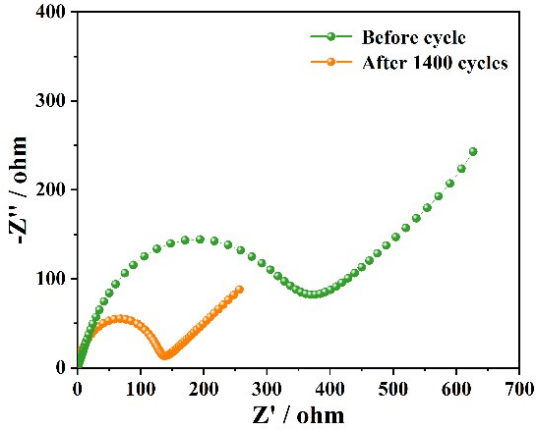

Figure S29 EIS curves of the flexible ZIBs before and after 1400 charge/discharge cycles.

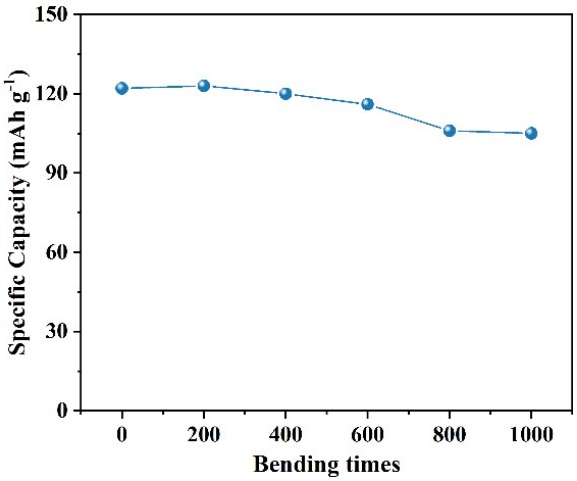

Figure S30 Specific capacities of flexible ZIBs during bending cycles.

Table S1 The cycle performance of the recently reported ZVO cathodes of ZIBs.

Materials	Voltage range	Zn^{2+} diffusion coefficient	Retention	Cycles	Current density	Ref.
ZVO/Mxene	0-1.8 V	10^{-7} to 10^{-8} cm^2 s^{-1}	84%	14000	10 A g^{-1}	This Work
			88%	1200	2 A g^{-1}	
			95%	60	0.1 A g^{-1}	
ZVO	0.2-1.8 V	≈10^{-9} to 10^{-10} cm^2 s^{-1}	68%	300	0.2 A g^{-1}	1
HfO_2-coated ZVO	0.2-1.8 V		84%	1000	10 A g^{-1}	2
			90%	100	0.1 A g^{-1}	
β-$AgVO_3$	0.4-1.3 V	10^{-9} cm^2 s^{-1}	77.86%	1000	2 A g^{-1}	3
			84%	200	0.1 A g^{-1}	
ZVO NSs@OCNT	0.2-1.8 V	≈10^{-9} to 10^{-10} cm^2 s^{-1}	75.3%	2000	5 A cm^{-3}	4
			88.6%	2000	1 A cm^{-3}	
ZVO nanowires	0.2-1.8 V	10^{-11} to 10^{-10} cm^2 s^{-1}	77%	700	2 A g^{-1}	5
V-doped MnO_2/ZVO	1.0-1.8 V		99%	100	0.1 A g^{-1}	6
VEG@MXene	0.2-1.6 V	10^{-9} to 10^{-10} cm^2 s^{-1}	85.2%	3000	10 A g^{-1}	7
			89.7%	1000	5 A g^{-1}	
			90.7%	200	0.5 A g^{-1}	
V_2O_3@C	0.3-1.6 V	4.39×10^{-10} to 4.15×10^{-9} cm^2 s^{-1}	61.3%	1800	10 A g^{-1}	8
ZVNW-CC	0.2-1.6 V	10^{-9} to 10^{-11} cm^2 s^{-1}	96.7%	1010	1 A g^{-1}	9
			93.7%	250	0.5 A g^{-1}	
			80%	650	0.2 A g^{-1}	
$Na_5V_{12}O_{32}$@graphene	0.2-1.6 V		85.7%	4400	5 A g^{-1}	10
			96.4%	340	0.3 A g^{-1}	
V_6O_{13}	0.3-1.4 V		78.9%	1000	10 A g^{-1}	11

References

1. C. Xia, J. Guo, Y. Lei, H. Liang, C. Zhao and H. N. Alshareef, *Adv. Mater.*, 2018, **30**, 1705580.
2. J. Guo, J. Ming, Y. Lei, W. Zhang, C. Xia, Y. Cui and H. N. Alshareef, *ACS Energy Lett.*, 2019, **4**, 2776-2781.
3. H. Liu, J.-G. Wang, H. Sun, Y. Li, J. Yang, C. Wei and F. Kang, *J. Colloid Interface Sci.*, 2020, **560**, 659-666.
4. Z. Pan, J. Yang, J. Yang, Q. Zhang, H. Zhang, X. Li, Z. Kou, Y. Zhang, H. Chen, C. Yan and J. Wang, *ACS Nano*, 2020, **14**, 842-853.
5. H. Cao, C. Peng, Z. Zheng, Z. Lan, Q. Pan, U. G. Nielsen, P. Norby, X. Xiao and S. Mossin, *Electrochimic. Acta*, 2021, **388**, 138646.
6. L. Ren, G. Yu, H. Xu, W. Wang, Y. Jiang, M. Ji and S. Li, *ACS Sustain. Chem. Eng.*, 2021, **9**, 12223-12232.
7. X. Li, X. Zhu, Z. Cao, Z. Xu, J. Shen and M. Ye, *Small*, 2022, **18**, 2105325.
8. Y. Ma, Y. Qi, Y. Niu, Y. Liu, S. Bao and M. Xu, *Inorg. Chem. Front.*, 2022, **9**, 2706-2713.
9. Y. Cui, Y. Ding, L. Guo, C. Guo, Y. Liu, Y. Bai, G. Li and K. Wang, *Energy Mater.*, 2023, **3**, 300023.
10. L. Rao, Z. Zhou, H. Liu, W. Peng, Y. Li, F. Zhang and X. Fan, *J. Colloid Interface Sci.*, 2023, **629**, 473-481.
11. Y. Li, H. Ba, Z. Wang, S. Wu, Y. Shang, S. Huang and H. Y. Yang, *Mater. Today Energy*, 2024, **39**, 101460.